

Regional marine boundary layer aerosol size distributions in the Indian, Atlantic, and Pacific Oceans: A comparison of INDOEX measurements with ACE-1, ACE-2, and Aerosols99

Timothy S. Bates,^{1,2,3} Derek J. Coffman,^{1,2} David S. Covert,^{2,3} and Patricia K. Quinn^{1,2}

Received 2 August 2001; revised 13 November 2001; accepted 27 November 2001; published 6 September 2002.

[1] Aerosol number size distributions were measured aboard the R/V *Ronald H. Brown* during the Indian Ocean Experiment (INDOEX) 1999 Intensive Field Phase (IFP) using a differential mobility particle sizer (DMPS) and an aerodynamic particle sizer (APS), covering a size range from 0.02 to 7 μm geometric diameter at 55% relative humidity (RH). The Indian Ocean marine boundary layer (MBL) aerosol number size distributions measured during the 1999 IFP were categorized into eight air mass source regions based on air mass back trajectories. The number and volume size distributions in these eight regions were distinctly different as a result of the different aerosol sources, meteorological conditions during transport, and time spent in the MBL. The aerosol sampling and data reduction during INDOEX were similar to that used during the Aerosol Characterization Experiment (ACE)-1 (Mid-Pacific Ocean 37°N to 32°S and Southern Ocean south of Tasmania, Australia), ACE-2 (North Atlantic Ocean west of Portugal and North Africa), and Aerosols99 (Atlantic Ocean transit from Norfolk, USA to Cape Town, South Africa) thus facilitating comparisons of the number and volume size distributions from these different experiments. The combined data set, summarized in this paper, provides regional aerosol parameters for comparison with global climate models and satellite retrieval algorithms. **INDEX TERMS:** 0305 Atmospheric Composition and Structure: Aerosols and particles (0345, 4801); 0322 Atmospheric Composition and Structure: Constituent sources and sinks; 0365 Atmospheric Composition and Structure: Troposphere—composition and chemistry; 0368 Atmospheric Composition and Structure: Troposphere—constituent transport and chemistry; **KEYWORDS:** aerosol, INDOEX, size distributions, ACE

Citation: Bates T. S., D. J. Coffman, D. S. Covert, and P. K. Quinn, Regional marine boundary layer aerosol size distributions in the Indian, Atlantic, and Pacific Oceans: A comparison of INDOEX measurements with ACE-1, ACE-2, and Aerosols99, *J. Geophys. Res.*, 107(D19), 8026, doi:10.1029/2001JD001174, 2002.

1. Introduction

[2] Global climate models (GCMs) and satellite retrieval algorithms require aerosol chemical composition as a function of size to calculate aerosol radiative effects and cloud condensation nuclei number. In most cases, the size distribution is prescribed in the model or algorithm because of the difficulty in representing the many processes controlling the size distribution (e.g., nucleation, preexisting size distribution, condensation, cloud processing, wet and dry deposition). Multiwavelength satellite retrievals can be used to derive aerosol size distributions but still require a large number of assumptions [King *et al.*, 1999]. Field campaigns provide a direct measurement of aerosol properties that can

be used to constrain, test, validate, and refine the assumptions used in GCMs and satellite retrieval algorithms. Although the field campaigns cover a very limited time and space, the data can be binned to provide regional aerosol properties based on location and air mass back trajectories.

[3] During February–March 1999, the Indian Ocean Experiment (INDOEX) Intensive Field Phase (IFP) quantified the atmospheric chemistry, aerosol properties, and radiation budget over the Indian Ocean [Ramanathan *et al.*, 2001]. Measurements aboard the R/V *Ronald H. Brown* covered the Southern and Northern Indian Ocean, Arabian Sea, and Bay of Bengal (Figure 1). Reported here are aerosol number and volume size distributions measured aboard the ship summarized by air mass source regions. The regions were defined using air mass back trajectories calculated for the ship's position at six hour intervals with the hybrid single-particle Lagrangian integrated model HY-SPLIT 4 based on the National Centers for Environmental Prediction (NCEP) global wind fields [Draxler, 1992; <http://www.noaa.gov/ready-bin/fnl.pl>]. The regions conform to the meteorological regimes defined for the study area by W. P. Ball *et al.* (Bulk and size-segregated aerosol compo-

¹NOAA/Pacific Marine Environmental Laboratory (PMEL), Seattle, Washington, USA.

²The Joint Institute for the Study of the Atmosphere and Ocean (JISAO), University of Washington, Seattle, Washington, USA.

³Department of Atmospheric Sciences, University of Washington, Seattle, Washington, USA.

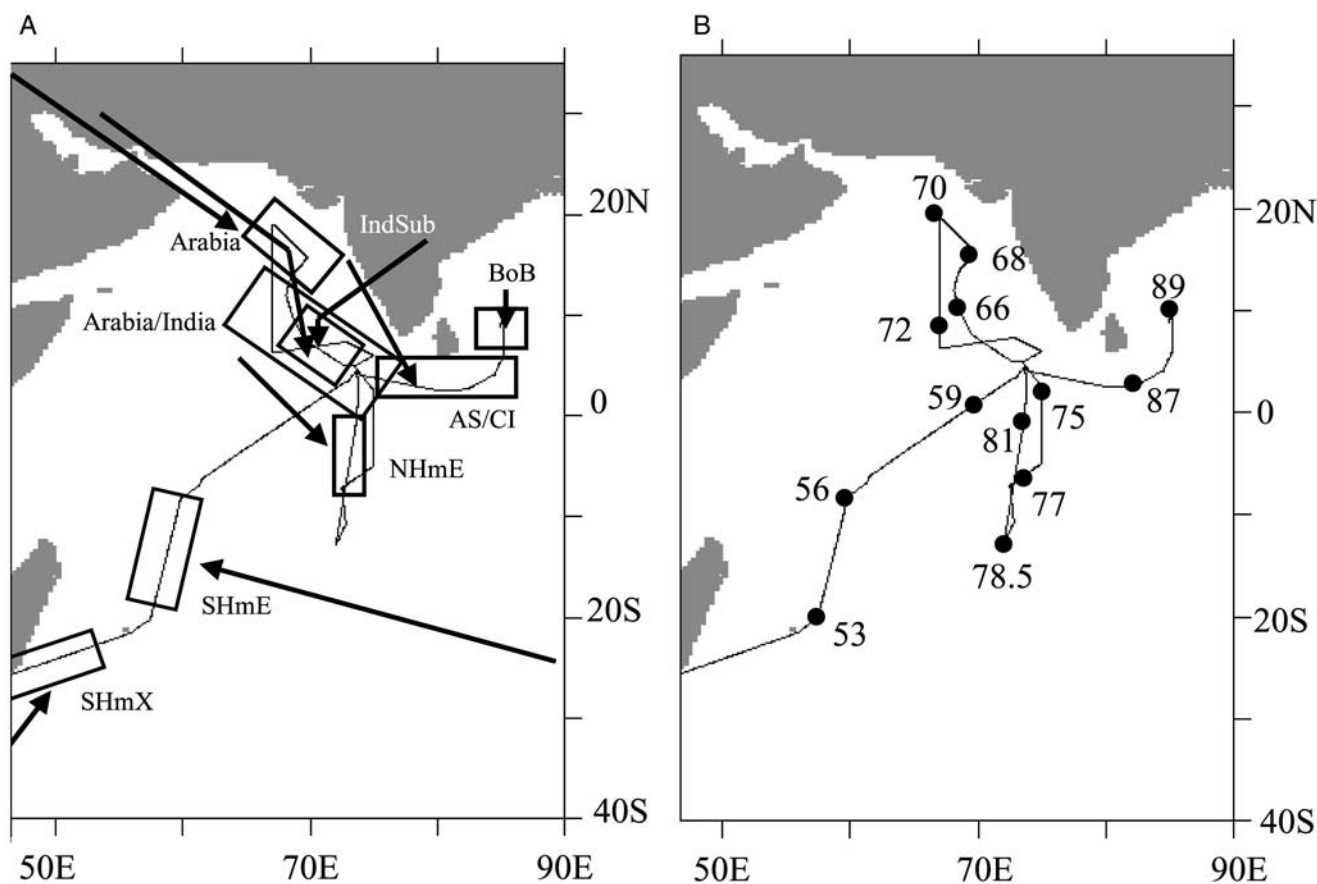


Figure 1. (a) INDOEX study area showing cruise track (light line), regions over which size distributions were averaged (darker squares), and generalized 6-day back trajectories arriving at 500 m elevation (heavy line). The SHmX region extended to Cape Town and the SHmX trajectory extended into the South Atlantic Ocean. (b) *Ronald H. Brown* cruise track during INDOEX. The circles and numbers are the location of the ship at the beginning of that day of year (note 78.5 is midday).

sition: Continental impacts during INDOEX 1999, submitted to *Journal of Geophysical Research*, 2001, hereinafter referred to as Ball et al., submitted manuscript, 2001). [Southern Hemisphere maritime extra-tropical (SHmX), Southern Hemisphere maritime equatorial (SHmE), Northern Hemisphere maritime equatorial (NHmE), Northern Hemisphere continental tropical (NHcT), Northern Hemisphere continental extra-tropical (NHcX), and Northern Hemisphere continental (NHc)] and the aerosol source regions defined by Quinn et al. [2002].

[4] The particle size distributions reported here are in terms of geometric diameter at 55% relative humidity (RH). A major goal of our measurement program is to quantify the relationships between the chemical, physical, and optical properties of the aerosol [Quinn et al., 2002]. To reduce the uncertainties in these comparisons we attempt to measure all the aerosol properties at a common controlled RH (55%). The size distributions can be adjusted to other relative humidities with published growth factors [e.g., Swietlicki et al., 2000].

2. Methods

2.1. Inlet

[5] Aerosol sampling and analysis methods were similar to those used in the Aerosol Characterization Experiment

(ACE)-1 [Bates et al., 1998a, 1998b; Quinn et al., 1998], ACE-2 [Bates et al., 2000; Quinn et al., 2000], and Aerosols99 [Bates et al., 2001; Quinn et al., 2001]. Aerosol particles were sampled 18m above the sea surface through a heated mast that extended 5 m above the aerosol measurement container. The mast was capped with a cone-shaped inlet nozzle that was rotated into the relative wind to maintain nominally isokinetic flow and minimize the loss of supermicron particles. Air was drawn through the 5 cm diameter inlet nozzle at $1 \text{ m}^3 \text{ min}^{-1}$ and down the 20 cm diameter mast. The lower 1.5 m of the mast were heated to dry the aerosol to a RH of $55 \pm 5\%$. This allowed for constant instrumental size cuts through variations in ambient RH. Fifteen 1.9 cm diameter electrically conductive polyethylene or stainless-steel sampling tubes extend into this heated zone to direct the air stream at flows of 30 l min^{-1} to the various aerosol sizing/counting instruments and impactors.

2.2. Inlet Efficiency

[6] Accurate measurements of aerosol properties by sampling instrumentation require that the particles be transported with known efficiencies from the atmosphere to the instruments. For particles with diameters between 5 and 1000 nm diffusion and impaction losses can be minimized

relatively easily. Comparisons of the total particle count ($D_p > 3$ nm) during ACE-1 between the NCAR C-130 airplane, ground stations, and ship agreed to within 20% when sampling in the same air mass [Weber *et al.*, 1999]. A similar comparison during the Indian Ocean Experiment (INDOEX) showed agreement to within 5% [Clarke *et al.*, 2002]. These differences are on the order of the atmospheric variability over the distance between platforms and the sample flow errors implying that inlet losses in this size range are minimal.

[7] Assessing the inlet efficiency for particles larger than ~ 1000 nm is more difficult. Comparisons of marine boundary layer (MBL) particle extinction based on in situ measurements and total column measurements (NASA Ames suntracking sunphotometer [Livingston *et al.*, 2000]) during ACE-2 agreed to within the uncertainties of the measurements and calculations, however those uncertainties were quite high. To better characterize the transmission efficiency of the shipboard sampling inlet for super-micron particles, the mast was tested after INDOEX in the Kirsten Wind Tunnel at the University of Washington. The Kirsten Wind Tunnel is a subsonic, closed circuit, double return wind tunnel. The tunnel has a test section with a rectangular $2.9 \text{ m} \times 4.4 \text{ m}$ cross-section that is 3.6 m long. The mast was mounted under the wind tunnel with the rotating top cone extending into the center of this test section. Two sets of 5.4 m-diameter seven-bladed propellers moved the air through the test section at speeds of 7 to 20 m/s for the mast tests. Polyethylene glycol (PEG - 400 molecular weight mixed as a 10% by volume solution in distilled water) aerosol particles were generated using a pressurized tank and spray nozzle immediately downwind of the mast. Although NaCl particles would have better simulated marine aerosol, concern about corrosion in the wind tunnel precluded their use. Aerosol size distributions were measured in the tunnel in 46 size bins with midpoint diameters ranging from 0.56 to 14 μm diameter using Aerodynamic Particle Sizers (APS model 3320, TSI, St. Paul, MN). The aerosol generator was operated for approximately 1 min every 5 min to maintain a steady concentration of approximately 500 particles per cm^3 ($\pm 5\%$ over a 2 hour run series) with diameters greater than 0.56 μm . The generated number size distributions were monomodal with a mean modal aerodynamic diameter of approximately 1 μm . Data were collected over 5-min intervals. The variability between runs under identical conditions (e.g., mast angle, wind speed) increased with particle diameter from $<2\%$ below 2 μm to $<10\%$ at 5 μm . Data collected in bins $>6.5 \mu\text{m}$ were within the instrument noise level due to Poisson counting statistics.

[8] Transmission efficiency tests were conducted with 2 APS instruments. The instruments were initially placed side-by-side with isokinetic inlets extending into the tunnel and parallel to the wind at the mast inlet height. After quantifying the relative responses of the 2 instruments, one instrument was moved to the base of the mast. The size distributions measured with the APS at the base of the mast were then normalized with the distribution measured with the short isokinetic inlet near the mast inlet to calculate transmission efficiency. Tests were conducted at different angles (0, 15, 30, 45, 60, and 90 degrees) between the wind vector and the mast inlet cone axis, at different wind speeds

(7, 10, 15, and 20 m/s), at different airflows down the mast (30, 220, 700, 1000, and 1200 L/m), and with different sampling tube locations at the base of the mast. The only one of these parameters that affected the transmission efficiency of the mast beyond the measurement uncertainties (10% below 5 μm diameter) was the angle between the wind and mast inlet cone. As the angle increased the transmission efficiency of particles decreased (Figure 2). At a 90 degree angle, the inlet transmitted only 60% of the particles in the 6 μm diameter size bin.

[9] During the field measurement campaigns the mast inlet was generally kept to within 15 degrees of the wind direction as described in the sampling protocol. Based on the wind tunnel tests, the transmission efficiency for particles with diameters less than 6.5 μm is greater than 95% under these conditions. The field data reported here have not been adjusted for mast inlet angles.

2.3. Aerosol Number Distributions and Concentrations Measured During INDOEX

[10] Total particle number concentrations were measured with a condensation particle counter (CPC, model 3010, TSI, St. Paul, MN) operated directly off one of the 1.9 cm sampling tubes. The same tube was used to supply ambient air to a differential mobility particle sizer (DMPS) located inside the humidity-controlled box at the base of the mast. The DMPS was a University of Vienna medium column unit [Winklmayr *et al.*, 1991], operating with a negative particle charge, connected to CPC. Data were collected in 27 size bins with midpoints ranging from 22 and 900 nm diameter. The DMPS operated with an aerosol flow rate of 0.5 L/min and a sheath airflow rate of 5 L/min. The sheath air was humidified to 55% RH. Mobility distributions were collected every 15 min.

[11] The DMPS data were edited to eliminate periods of calibration and instrument malfunction and periods of ship contamination (based on relative wind and high and rapid changes in CN counts). The data were corrected for diffusional losses [Covert *et al.*, 1997] and size dependent counting efficiencies [Wiedensohler *et al.*, 1997] based on intercalibration exercises prior to ACE-1 and ACE-2. The mobility distributions were then converted to number-size distributions using the inversion routine of Stratman and Wiedensohler [1997]. The accuracy of both the particle sizing and the number of particles in each size bin depends on the stability of the flow rates. Three of the four DMPS flows (CPC, Sheath, and Excess) were controlled independently. The DMPS inlet flow was the difference of these flows, nominally 10% of the sheath flow. The flow calibration involved setting the CPC flow and DMA sheath flow with an electronic bubble flowmeter. The excess flow was balanced with the sheath airflow such that the DMPS inlet flow was equal to the CPC flow. The inversion and evaluation of the DMPS data assumed the sheath and excess flows were equal and that the inlet flow equaled the CPC flow. The drift in the CPC, sheath, and excess flows was generally less than one percent during the cruise (mean $0.63 \pm 0.55\%$). This translates into a similar error in particle sizing of plus or minus a percent. However, a relative drift of 1% in the sheath to excess flow translates into a 10% change in the DMPS inlet flow and thus a 10% change in the number concentration. A change in the inlet flow also

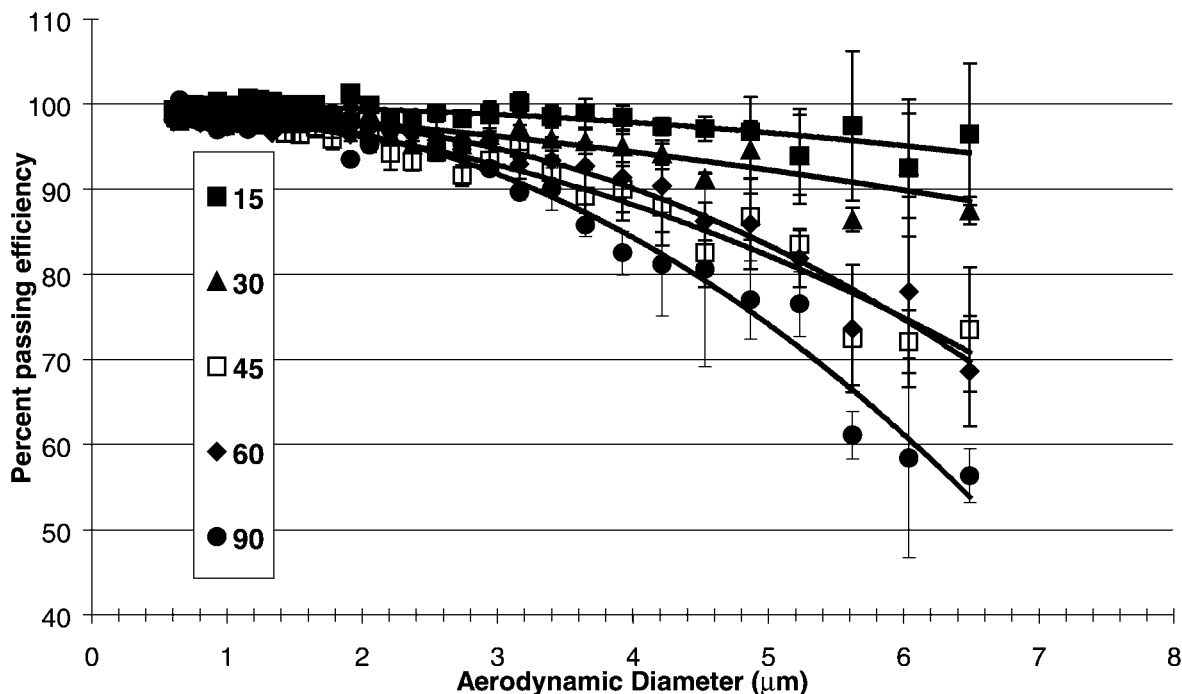


Figure 2. Percent transmission efficiency of the mast at different angles between the inlet nozzle and the wind direction. The vertical bars represent one standard deviation of the mean efficiency in each APS size bin. The curves are a second-order polynomial fit through the data at each angle.

results in a change in the transfer function of the DMA which compounds this error, e.g., for this case the combined error is on the order of 15%. During INDOEX, the integrated number concentration from the DMPS operated at 55% RH averaged $6.5 \pm 7.1\%$ lower than the total number measured by the CPC. To correct for this differential number concentration error, the DMPS data reported have been normalized using the 30-min average ratio of the total number concentration to the integrated DMPS number concentration.

[12] Another one of the 1.9 cm tubes was connected to an APS (model 3320, TSI) located in the humidity-controlled box at the base of the mast. The APS measured the number size distribution between 0.6 and 9.6 μm aerodynamic diameter. Although the intent was to measure this distribution at 55% RH, comparisons between gravimetrically determined mass at 33% RH and mass derived from the APS revealed that the heat from the instrument effectively dried the coarse mode salt aerosol to below its efflorescence point. The APS data were converted from aerodynamic diameters at a measurement RH below the efflorescence point of sea salt to geometric diameters at 55% RH using calculated densities and the water masses associated with the inorganic ions at 33 and 55% RH. The densities and associated water masses were calculated with a thermodynamic equilibrium model (AeRho) using the measured chemical data [Quinn *et al.*, 2002].

[13] The combined DMPS and APS number distributions were converted to surface area distributions. An interactive routine was then used to fit lognormal curves to the Aitken, accumulation, and coarse modes of the surface area distributions. The modal parameters were then converted to number and volume concentrations and geometric diameters

for the model number and volume size distributions, respectively (Table 1).

2.4. Aerosol Number Distributions and Concentrations from Previous Experiments

[14] The instrumentation used to measure aerosol number size distributions and concentrations aboard the ship in ACE-1, ACE-2, and Aerosols99 have been described in detail previously [Bates *et al.*, 1998b, 2000, 2001]. The data have since been reanalyzed to adjust the distributions to a common humidity of 55%. The reanalyzed data are available to the community at <http://saga.pmel.noaa.gov/data/>.

[15] Aerosol number size distributions were measured aboard R/V *Discoverer* during ACE-1 [Bates *et al.*, 1998a] with the DMPSs at a “dry” (<10% RH) reference humidity. The integral of the number concentration was within $2 \pm 20\%$ of the total number concentration measured with an ultrafine CPC (UCPC, model 3025, TSI 3025) so no adjustment was made to the number distribution. The size distributions from the DMPS were adjusted to 55% based on a diameter growth factor of 1.2 measured during ACE-1 [Berg *et al.*, 1998]. The APS data during ACE-1 were collected at a humidity of approximately 40%. Based on the coarse mode size distribution and the data fit between the DMPS and APS, it appears that the APS data were collected at a humidity below the efflorescence point of sea salt, similar to the conditions during INDOEX. Thus the APS data were converted to geometric diameters at 55% RH using the same model and assumptions as used for the INDOEX data (see section 2.3).

[16] Aerosol number size distributions measured aboard R/V *Professor Vodyanitskiy* during ACE-2 [Bates *et al.*, 2000] were at an RH of approximately 45%. The integral of

Table 1. Average Modal Parameters for the Different Air Masses During the Four Cruises

Air Mass DOY Latitude ^a	Modal Parameter ^b	Aitken Number ^c	Accumulation Number ^c	Accumulation Volume ^c	Coarse Volume 1 ^c	Coarse Volume 2 ^c
<i>INDOEX (February–March 1999)</i>						
SHmX 43.6–50.3 34°S–22°S	<i>N</i> or <i>V</i> <i>D_{gN}</i> or <i>D_{gV}</i> σ	380 ± 190 0.038 ± 0.0044 1.5 ± 0.14	140 ± 30 0.14 ± 0.011 1.3 ± 0.034	0.33 ± 0.072 0.19 ± 0.014 1.3 ± 0.034	16 ± 6.5 3.2 ± 0.32 1.7 ± 0.19	
SHmE 54.3–55.5 15°S–10°S	<i>N</i> or <i>V</i> <i>D_{gN}</i> or <i>D_{gV}</i> σ	100 ± 86 0.066 ± 0.021 1.4 ± 0.096	77 ± 26 0.20 ± 0.015 1.4 ± 0.12	0.55 ± 0.19 0.29 ± 0.023 1.4 ± 0.12	6.7 ± 3.8 3.1 ± 0.32 1.9 ± 0.10	
IndSub NHcT 63.9–66.5	<i>N</i> or <i>V</i> <i>D_{gN}</i> or <i>D_{gV}</i> σ	960 ± 340 0.12 ± 0.014 1.6 ± 0.077	530 ± 110 0.28 ± 0.021 1.4 ± 0.046	9.7 ± 2.0 0.38 ± 0.027 1.4 ± 0.046	3.9 ± 0.86 2.4 ± 0.12 1.7 ± 0.023	
Arabia NHcX 68.1–69.1	<i>N</i> or <i>V</i> <i>D_{gN}</i> or <i>D_{gV}</i> σ	640 ± 480 0.050 ± 0.011 1.4 ± 0.093	450 ± 66 0.14 ± 0.011 1.7 ± 0.11	2.6 ± 0.39 0.35 ± 0.028 1.7 ± 0.11	10 ± 3.4 2.9 ± 0.11 1.7 ± 0.044	
Arabia/India NHcX/NHcT 71.4–74.6	<i>N</i> or <i>V</i> <i>D_{gN}</i> or <i>D_{gV}</i> σ	380 ± 380 0.070 ± 0.019 1.4 ± 0.10	670 ± 180 0.20 ± 0.012 1.5 ± 0.050	6.2 ± 1.6 0.35 ± 0.021 1.5 ± 0.050	9.2 ± 1.9 2.5 ± 0.20 1.7 ± 0.043	
NHmE 79.5–81.0 8°S–1°S	<i>N</i> or <i>V</i> <i>D_{gN}</i> or <i>D_{gV}</i> σ	120 ± 80 0.060 ± 0.016 1.5 ± 0.11	280 ± 75 0.18 ± 0.021 1.6 ± 0.050	2.2 ± 0.60 0.34 ± 0.039 1.6 ± 0.050	12 ± 1.7 3.0 ± 0.13 1.8 ± 0.57	
AS/CI NHcT 85.6–88.7	<i>N</i> or <i>V</i> <i>D_{gN}</i> or <i>D_{gV}</i> σ	310 ± 230 0.085 ± 0.017 1.6 ± 0.084	360 ± 110 0.23 ± 0.0063 1.4 ± 0.059	4.2 ± 1.3 0.34 ± 0.0095 1.4 ± 0.059	2.1 ± 1.1 2.1 ± 0.27 1.6 ± 0.039	
BoB NHcT 88.8–89.5	<i>N</i> or <i>V</i> <i>D_{gN}</i> or <i>D_{gV}</i> σ	370 ± 29 0.13 ± 0.0029 1.5 ± 0.040	540 ± 39 0.27 ± 0.0029 1.3 ± 0.0059	7.6 ± 0.54 0.34 ± 0.0036 1.3 ± 0.0059	1.1 ± 0.067 1.9 ± 0.016 1.6 ± 0.031	
<i>Aerosols99 (January–February 1999)</i>						
N. America NHcT 16.7–17.0	<i>N</i> or <i>V</i> <i>D_{gN}</i> or <i>D_{gV}</i> σ	480 ± 120 0.042 ± 0.0023 1.5 ± 0.070	520 ± 140 0.21 ± 0.011 1.4 ± 0.028	3.7 ± 1.0 0.28 ± 0.015 1.4 ± 0.28	6.2 ± 3.1 1.1 ± 0.11 1.8 ± 0.48	25 ± 7.3 3.6 ± 0.23 1.6 ± 0.11
NHmT 17.5–22.4 31°N–17°N	<i>N</i> or <i>V</i> <i>D_{gN}</i> or <i>D_{gV}</i> σ	190 ± 58 0.035 ± 0.0053 1.5 ± 0.082	65 ± 19 0.17 ± 0.025 1.4 ± 0.11	0.32 ± 0.092 0.26 ± 0.038 1.4 ± 0.11	7.2 ± 3.2 2.0 ± 0.62 2.1 ± 0.52	24 ± 8.7 3.6 ± 0.37 1.7 ± 0.14
Mineral dust NHcT 23.3–25.6	<i>N</i> or <i>V</i> <i>D_{gN}</i> or <i>D_{gV}</i> σ	240 ± 40 0.046 ± 0.0027 1.4 ± 0.035	130 ± 25 0.15 ± 0.0067 1.4 ± 0.030	0.34 ± 0.064 0.20 ± 0.0091 1.4 ± 0.030	8.8 ± 2.8 1.3 ± 0.24 1.9 ± 0.22	32 ± 6.9 2.7 ± 0.13 1.6 ± 0.063
<i>Aerosols99 (January–February 1999)</i>						
Biomass Burning NHcE 27.4–29.4	<i>N</i> or <i>V</i> <i>D_{gN}</i> or <i>D_{gV}</i> σ	240 ± 130 0.090 ± 0.017 1.5 ± 0.096	310 ± 78 0.19 ± 0.007 81.5 ± 0.034	2.6 ± 0.65 0.32 ± 0.013 1.5 ± 0.034	6.1 ± 2.2 2.5 ± 0.12 1.7 ± 0.059	
SHmE 30.0–35.9 6°S–24°S	<i>N</i> or <i>V</i> <i>D_{gN}</i> or <i>D_{gV}</i> σ	110 ± 34 0.057 ± 0.0067 1.4 ± 0.074	100 ± 30 0.21 ± 0.011 1.5 ± 0.072	1.0 ± 0.31 0.35 ± 0.019 1.5 ± 0.072	11 ± 4.3 3.2 ± 0.11 1.9 ± 0.066	
SHmT 35.9–38.7 24°S–32°S	<i>N</i> or <i>V</i> <i>D_{gN}</i> or <i>D_{gV}</i> σ	210 ± 40 0.052 ± 0.0036 1.5 ± 0.056	140 ± 25 0.21 ± 0.011 1.3 ± 0.032	1.0 ± 0.18 0.27 ± 0.014 1.3 ± 0.032	26 ± 3.3 3.6 ± 0.17 1.9 ± 0.13	
<i>ACE-2 (June–July 1997)</i>						
NHmT 178.5–185.1	<i>N</i> or <i>V</i> <i>D_{gN}</i> or <i>D_{gV}</i> σ	560 ± 250 0.042 ± 0.010 1.5 ± 0.40	120 ± 26 0.22 ± 0.016 1.4 ± 0.060	1.3 ± 0.26 0.33 ± 0.025 1.4 ± 0.060	d d d	
Mediterranean NHcT 187.4–188.5	<i>N</i> or <i>V</i> <i>D_{gN}</i> or <i>D_{gV}</i> σ	5100 ± 1700 0.12 ± 0.018 1.6 ± 0.060	200 ± 65 0.31 ± 0.037 1.3 ± 0.081	4.4 ± 1.4 0.39 ± 0.046 1.3 ± 0.081	d d d	
W. Europe NHcT 190.6–192.4	<i>N</i> or <i>V</i> <i>D_{gN}</i> or <i>D_{gV}</i> σ	910 ± 600 0.11 ± 0.018 1.7 ± 0.086	540 ± 160 0.27 ± 0.019 1.4 ± 0.045	8.4 ± 2.5 0.36 ± 0.025 1.4 ± 0.045	d d d	
Iberian Coast NHcT 193.9–201.0	<i>N</i> or <i>V</i> <i>D_{gN}</i> or <i>D_{gV}</i> σ	3800 ± 2400 0.090 ± 0.018 1.6 ± 0.13	370 ± 160 0.31 ± 0.031 1.3 ± 0.068	8.3 ± 3.5 0.39 ± 0.038 1.3 ± 0.068	d d d	
<i>ACE-1 (October–December 1995)</i>						
NHmT 288.5–291.0 37°N–27°N	<i>N</i> or <i>V</i> <i>D_{gN}</i> or <i>D_{gV}</i> σ	200 ± 71 0.044 ± 0.0043 1.3 ± 0.12	70 ± 22 0.19 ± 0.014 1.5 ± 0.11	0.49 ± 0.16 0.29 ± 0.022 1.5 ± 0.11	9.2 ± 7.3 3.8 ± 0.36 1.7 ± 0.46	
SHmE 297.5–300.0 4°N–9°S	<i>N</i> or <i>V</i> <i>D_{gN}</i> or <i>D_{gV}</i> σ	160 ± 29 0.056 ± 0.0060 1.4 ± 0.060	120 ± 14 0.19 ± 0.0088 1.4 ± 0.074	0.72 ± 0.082 0.26 ± 0.012 1.4 ± 0.074	17 ± 3.8 3.5 ± 0.13 1.5 ± 0.049	

Table 1. (continued)

Air Mass DOY Latitude ^a	Modal Parameter ^b	Aitken Number ^c	Accumulation Number ^c	Accumulation Volume ^c	Coarse Volume 1 ^c	Coarse Volume 2 ^c
<i>ACE-1 (October–December 1995)</i>						
SHmT	<i>N</i> or <i>V</i>	210 ± 94	83 ± 38	0.53 ± 0.24	11 ± 4.5	
302.0–305.0	<i>D_{gN}</i> or <i>D_{gV}</i>	0.045 ± 0.0050	0.19 ± 0.014	0.27 ± 0.020	4.3 ± 0.86	
20°S–32°S	σ	1.4 ± 0.11	1.4 ± 0.074	1.4 ± 0.074	2.0 ± 0.53	
SHmX	<i>N</i> or <i>V</i>	260 ± 170	72 ± 32	0.16 ± 0.070	23 ± 15	
320.0–346.0	<i>D_{gN}</i> or <i>D_{gV}</i>	0.036 ± 0.0081	0.13 ± 0.022	0.19 ± 0.032	3.0 ± 0.39	
41°S–55°S	σ	1.4 ± 0.25	1.4 ± 0.10	1.4 ± 0.10	2.0 ± 0.18	

^aDOY: Dates are given as day of year (DOY) where noon on 1 February equals DOY 32.5 UTC. Marine air masses also include the meridional sampling limits. All ACE-2 data reported here were collected between 30°N and 41°N, 7°W and 15°W.

^b*N* (cm⁻³), *V* (μm³cm⁻³), *D* (geometric at 55% RH) (μm).

^cModal parameters were calculated from lognormal fits to the surface area size distribution. ± refers to atmospheric variability in the air mass.

^dThe coarse mode data from ACE-2 could not be fit with a lognormal curve because of the open-ended distribution.

the number concentrations was $69 \pm 4\%$ of the total number concentration measured with a TSI 3025 CPC. In a manner similar to the INDOEX data reduction, the number size distributions were normalized using the 30-min average ratio of the total number concentration to the integrated DMPS number concentration. The size distributions from the DMPS were adjusted to 55% based on growth factors (1.05) measured during ACE-2 [Swietlicki *et al.*, 2000]. Based on the coarse mode size distribution and the data fit between the DMPS and APS, it appears that the APS data were collected at a humidity above the efflorescence point of sea salt. Thus no RH adjustment has been made to the data. The data were converted to geometric diameters using calculated densities and the water masses associated with the inorganic ions at 55% RH. The densities and associated water masses were calculated with AeRho using the measured chemical data. A TSI model 3310 APS was used for both ACE-1 and ACE-2. Although this instrument sizes particles between 0.8 and 10 μm, data at diameters larger than 4 μm were discarded due to interferences from phantom counts.

[17] The aerosol instrumentation and sampling humidities during Aerosols99 [Bates *et al.*, 2000] were the same as during INDOEX. Data reduction followed similar procedures. During Aerosols99, the integrated number concentration from the DMPS operated at 55% RH averaged $18 \pm 10\%$ lower than the total number measured by the TSI 3010. The DMPS data were normalized using the 30-min average ratio of the total number concentration to the integrated DMPS number concentration. The APS data were converted to geometric diameters at 55% RH using the same model and assumptions used for the INDOEX data (see section 2.3). The super-micron size mode during Aerosols99 and INDOEX were measured with a TSI model 3320 APS. The improved optical system in the 3320 greatly reduced the previous problem of phantom counts. The data reported here for Aerosols and INDOEX thus extend to 7 μm, the upper limit of the inlet transmission efficiency tests (see section 2.2).

3. Results and Discussion

3.1. Aerosol Number/Volume Distributions During the INDOEX 1999 IFP

[18] The INDOEX IFP took place during the dry winter monsoon season that is characterized by large-scale sub-

sidence over the Indian subcontinent and northeasterly flow from the continent over the Northern Indian Ocean (J. A. Coakley *et al.*, unpublished manuscript, 2000). This type of NHcT air mass (Ball *et al.*, submitted manuscript, 2001) was sampled at the ship from DOY 63.9 to 66.5 [All references to time are reported here in UTC. Dates are given as Day of Year (DOY) where noon on 1 February equals DOY 32.5]. The aerosol volume distributions (Figure 3a; Table 1) were dominated by submicron accumulation mode particles with a volume mean diameter of 0.38 ± 0.027 μm. The submicron aerosol advecting off the continent was composed primarily (>70% by mass) of nonsea-salt (nss) sulfate aerosol, which includes nss SO₄²⁻, NH₄⁺, and H₂O at 55% RH [Quinn *et al.*, 2002]. The additional presence of black carbon and nss potassium are indicative of a biomass or biofuel combustion source [Quinn *et al.*, 2002; Ball *et al.*, submitted manuscript, 2001].

[19] A NHcX air mass from Arabia that was sampled at the ship between DOY 68.1 and 69.1 (Figure 1) had a distinctly different aerosol number and volume distribution (Figure 3b). The number distribution was dominated by an Aitken mode aerosol with a mean diameter of 0.050 ± 0.011 μm while the volume distribution was dominated by the coarse mode aerosol with a mean diameter of 2.9 ± 0.11 μm. Although nss sulfate was still the dominant chemical component (approximately 60%) of the submicron aerosol, the fraction of particulate organic matter (POM ≈ 15%) and inorganic oxidized material (IOM ≈ 20%) was much higher than that found in the air mass from the Indian Subcontinent [Quinn *et al.*, 2002]. POM is defined here as the organic carbon concentration multiplied by 1.6 to account for the other elements in the organic aerosol [Quinn *et al.*, 2002]. IOM assumes that the soil dust and/or fly ash elements were present in the aerosol in their most common oxide form (Al₂O₃, SiO₂, CaO, K₂O, FeO, Fe₂O₃, TiO₂). Although the elemental concentrations alone are not sufficient to discriminate between soil dust and fly ash [Quinn *et al.*, 2002], the IOM in this NHcX air mass appeared to be soil dust based on spectral absorbance measurements (Ball *et al.*, submitted manuscript, 2001). The dominant small-diameter Aitken mode aerosol suggests the production of secondary aerosol from SO₂ and/or organic species that has experienced minimal growth by condensation or cloud processing in the two-day transit over the Arabian Sea to the ship. The volume distribution was dominated by the coarse mode aerosol that was a mixture of sea salt (≈70%) and soil dust

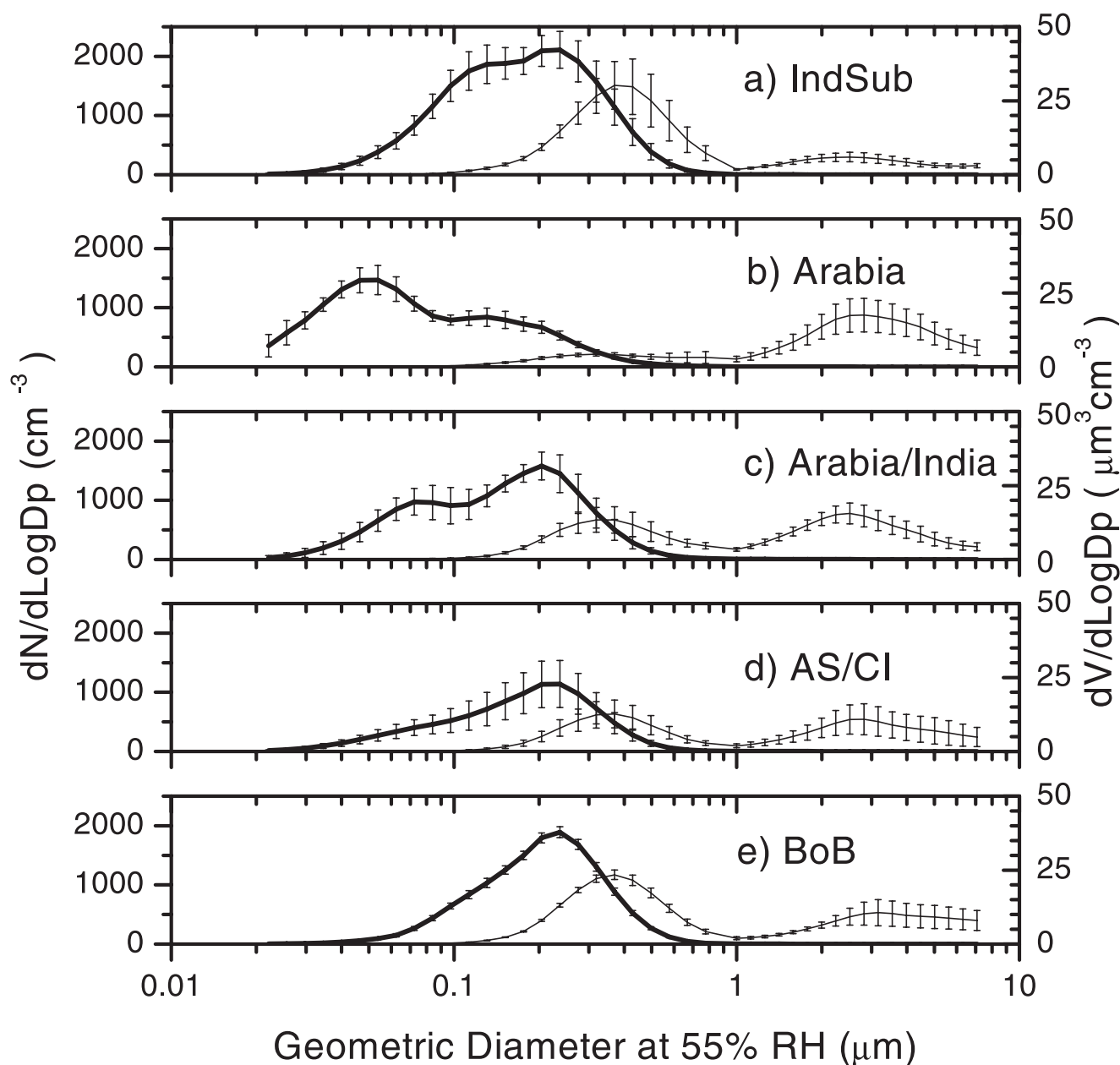


Figure 3. Number (heavy line) and volume (light line) distributions at 55% RH for 5 air mass source regions during INDOEX (Figure 1). The vertical bars represent one standard deviation in the mean number or volume in that bin size over the averaging period (Indian Subcontinent — 49 hr; Arabia — 21 hr; Arabia/Indian Subcontinent mix — 67 hr; Arabian Sea/Coastal India — 50 hr; Bay of Bengal — 16 hr).

($\approx 30\%$) [Quinn *et al.*, 2001; Ball *et al.*, submitted manuscript, 2001].

[20] Further south the ship sampled an air mass (NHc) that appeared to be a mix of NHcX air from Arabia in the MBL with NHcT air from India in the overlying free troposphere (FT). The aerosol number and volume distributions during this period (DOY 71.4–74.6, Figure 3c) reflected this mixture and the longer transit time from Arabia. The Aitken mode, though still present, had a larger diameter of $0.070 \pm 0.019 \mu\text{m}$. The accumulation mode was much larger than the NHcX air from Arabia in both number and diameter and was similar to the NHcT-Indian Subcontinent aerosol sampled previously (Figure 3a). The presence

of nss potassium (present in the NHcT air mass but not appreciably in the NHcX air mass) and a larger mass fraction of black carbon in the NHc air mass [Quinn *et al.*, 2002] supports the entrainment of NHcT air from the FT into the MBL. The volume distribution was nearly evenly divided into an accumulation mode that was mainly ($>70\%$) nss sulfate aerosol and a coarse mode that was composed of sea salt ($\approx 65\%$) and inorganic oxidized material ($\approx 25\%$) [Quinn *et al.*, 2002].

[21] South of the Indian Subcontinent the ship sampled (DOY 85.6–88.7) a NHcT air mass that had traveled along the west coast of India for the previous 6 days. Upper level (2500 m) trajectories crossed the Indian Subcontinent. This

Arabian Sea-Coastal India (AS/CI) air was essentially a dilute continental air mass based on the aerosol submicron chemistry [Quinn *et al.*, 2002] and the accumulation modal number and diameter (Figure 3d). Similarly, a NHcT air mass in the Bay of Bengal (BoB) sampled on DOY 88.8–89.5 had been over the ocean for more than 6 days. The dominant accumulation mode (Figure 3e) suggests a well-aged continental aerosol.

[22] During INDOEX the Intertropical Convergence Zone (ITCZ) drifted between the equator and 12°S. North of the ITCZ the ship sampled a convective and showery NHmE air mass between DOY 79.5 and 81 (Ball *et al.*, submitted manuscript, 2001). The aerosol number distribution consisted of both an Aitken and accumulation mode typical of marine air masses however the number concentration of the accumulation mode was significantly higher (280 versus 77) than that encountered in the SHmE (Figure 4b). Although this air mass had not been in contact with land during the previous 6 days, the presence of black carbon and nss potassium in the submicron mode [Quinn *et al.*, 2002] proves that there was a residual continental and/or anthropogenic component in this air mass. The volume distribution of this air mass was dominated by the coarse mode (Figure 4a) that was composed of sea salt ($\approx 80\%$) and inorganic oxidized material ($\approx 20\%$) [Quinn *et al.*, 2002].

[23] South of the ITCZ the aerosol size distributions (DOY 54.3–55.5) showed typical marine Aitken, accumulation, and coarse modes (Figure 4b). The number distribution was split between the Aitken and accumulation modes as is typical in equatorial air masses [Covert *et al.*, 1996]. The volume distribution was contained almost entirely within the coarse mode. In the SHmX air mass sampled south of Africa and Mauritius between DOY 43.6–50.3 (Figure 4c) the number size distribution was dominated by the Aitken mode. Six-day back trajectories extended well into the Southern Atlantic Ocean (50–60°S) as the subsiding air circled around the high pressure system south of Africa.

3.2. Marine Aerosol Number/Volume Distributions From ACE-1, ACE-2, and AEROSOLS99

[24] The aerosol number size distributions from Aerosols99 (Figures 5 and 6), ACE-2 (Figures 7 and 8) and ACE-1 (Figure 7) have been described previously in Bates *et al.* [2001], Bates *et al.* [2000], and Bates *et al.* [1998b], respectively. Here we compare the common regional features from these data sets.

[25] Air masses that were not in contact with land for >6 days are classified here as marine. The aerosol number size distributions in these air masses were dominated by well-defined Aitken ($20 \text{ nm} < D_p < 100 \text{ nm}$) and accumulation ($100 \text{ nm} < D_p < 800 \text{ nm}$) modes (Figures 5 and 7). During periods of convective mixing between the MBL and FT a third mode (nucleation mode, $5 \text{ nm} < D_p < 20 \text{ nm}$) was sometimes present [Covert *et al.*, 1996; Bates *et al.*, 1998b], evident here in the ACE-1 Southern Hemisphere extratropical (SHmX) (Figure 7e) and the ACE-2 Northern Hemisphere marine subtropical (NHmT) (Figure 7a) regions. The aerosol volume distribution was always dominated by the coarse mode with an average mean modal diameter of $\approx 3 \mu\text{m}$ (Table 1).

[26] The marine data from the ACE-1 Pacific Ocean measurements are summarized in 3 regions along the

cruise track from Seattle, USA to Hobart, Australia [Bates *et al.*, 1998a]: Northern Hemisphere subtropical (NHmT), Southern Hemisphere Equatorial (SHmE) and Southern Hemisphere subtropical (SHmT) (Table 1). The average total particle number in each region was $\approx 300 \text{ cm}^{-3}$ (Table 1) which was similar to the data reported for 3 Pacific Ocean cruises in 1992–1993 by Covert *et al.* [1996] ($280 \pm 50 \text{ cm}^{-3}$). In the large-scale subsidence of the subtropical Northern and Southern Hemisphere regions the number size distributions were dominated by the Aitken mode centered at $\approx 0.045 \mu\text{m}$ (55%RH) (Figures 7b, 7d). In the equatorial region the aerosol number was more evenly distributed between the Aitken and accumulation modes (Figures 7c and 5b). As described by Covert *et al.* [1996], the marine air masses associated with these aerosols had the longest mean residence time in the MBL or 5 days or more. With the longer MBL residence time the Aitken mode diameter can grow by condensation and coagulation [Raes *et al.*, 2000]. During ACE-1, the average diameter of the SHmE Aitken mode was $\approx 0.056 \mu\text{m}$ at 55% RH. The accumulation mode in all three ACE-1 Pacific Ocean regions was centered at $\approx 0.19 \mu\text{m}$ (55% RH). In the higher latitudes south of Australia (SHmX), the aerosol number was largely controlled by the postfrontal subsidence [Bates *et al.*, 1998b]. Cold fronts passing through the area every 2–3 days [Hainsworth *et al.*, 1998] frequently mixed nucleation mode particles into the MBL from the FT. The resulting short MBL residence times provided little time for particle growth. The mean modal diameters of the Aitken ($\approx 0.035 \mu\text{m}$ at 55% RH) and accumulation ($\approx 0.13 \mu\text{m}$ at 55% RH) modes (Figure 7e) were less than that measured in the subtropical and equatorial regions. However, the SHmX modal diameters measured in ACE-1 were very similar to the SHmX modal diameters measured in INDOEX (Figure 4c, Aitken and accumulation mean modal diameters of $\approx 0.038 \mu\text{m}$ and $0.14 \mu\text{m}$, respectively) suggesting similar processes controlling the size distributions.

[27] Large-scale weak subsidence in the Azores High provided Aitken mode particles from the FT to the MBL during ACE-2 [Bates *et al.*, 2000]. Although the mean size distribution shows a clear nucleation mode (Figure 7a) this feature was only present for a one half-day period in a region of broken convective clouds behind a weak frontal system [Bates *et al.*, 2000]. The mean diameter of the Aitken mode ($\approx 0.042 \mu\text{m}$ at 55% RH) was similar to the subtropical regions of the Pacific sampled during ACE-1. The accumulation mode mean diameter ($\approx 0.22 \mu\text{m}$), however, was higher than that measured during ACE-1, presumably due to enhanced condensational growth and liquid phase oxidation of soluble trace gases during cloud processing [Hoppel *et al.*, 1986].

[28] In contrast to the NHmT aerosol measured during ACE-2, the Aitken and accumulation modes measured in the Azores High during Aerosols99 (Figure 5a) had much smaller mean diameters ($\approx 0.035 \mu\text{m}$ and $0.17 \mu\text{m}$, respectively). Although calculated air mass back trajectories suggest the aerosol spent 3–6 days in the MBL, rainfall throughout this region and mixing induced from an easterly wave in the trade winds [Bates *et al.*, 2001] suggest a much shorter MBL residence time. Farther south in the subtropical high over the South Atlantic, the aerosol size distributions

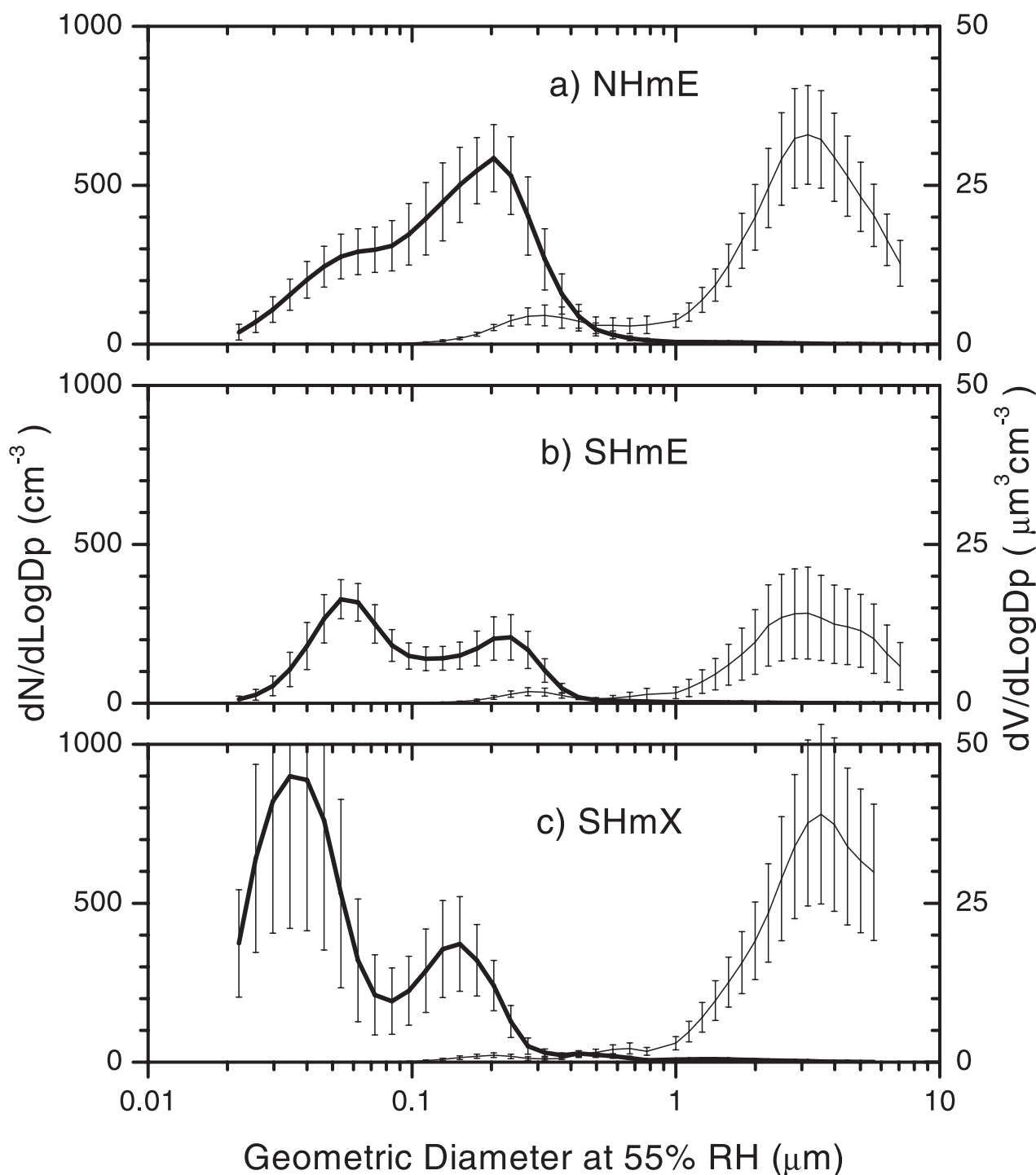


Figure 4. Number (heavy line) and volume (light line) distributions at 55% RH for 3 marine air mass source regions during INDOEX (Figure 1). The vertical bars represent one standard deviation in the mean number or volume in that bin size over the averaging period (N. Hemisphere marine Equatorial — 30 hr; S. Hemisphere marine Equatorial — 20 hr; S. Hemisphere marine Extra-tropical — 108 hr).

suggest longer MBL residence times (Figures 5b, 5c). The Aitken mode mean diameters in the SHmE and SHmT regions were $\approx 0.057 \mu\text{m}$ and $0.052 \mu\text{m}$, respectively. In the SHmE region the aerosol number was nearly evenly split between the Aitken and accumulation modes, similar to that observed in the Pacific (ACE-1, Figure 7c) [Covert *et al.*, 1996] and Indian (INDOEX, Figure 4b) Oceans. In the

SHmT region the Aitken mode was dominant, similar to the ACE-1 SHmT Pacific Ocean data.

3.3. Continental Aerosol Number/Volume Distributions from ACE-1, ACE-2, and AEROSOLS99

[29] The modified continental aerosol size distributions measured in the MBL reflected the source regions, mete-

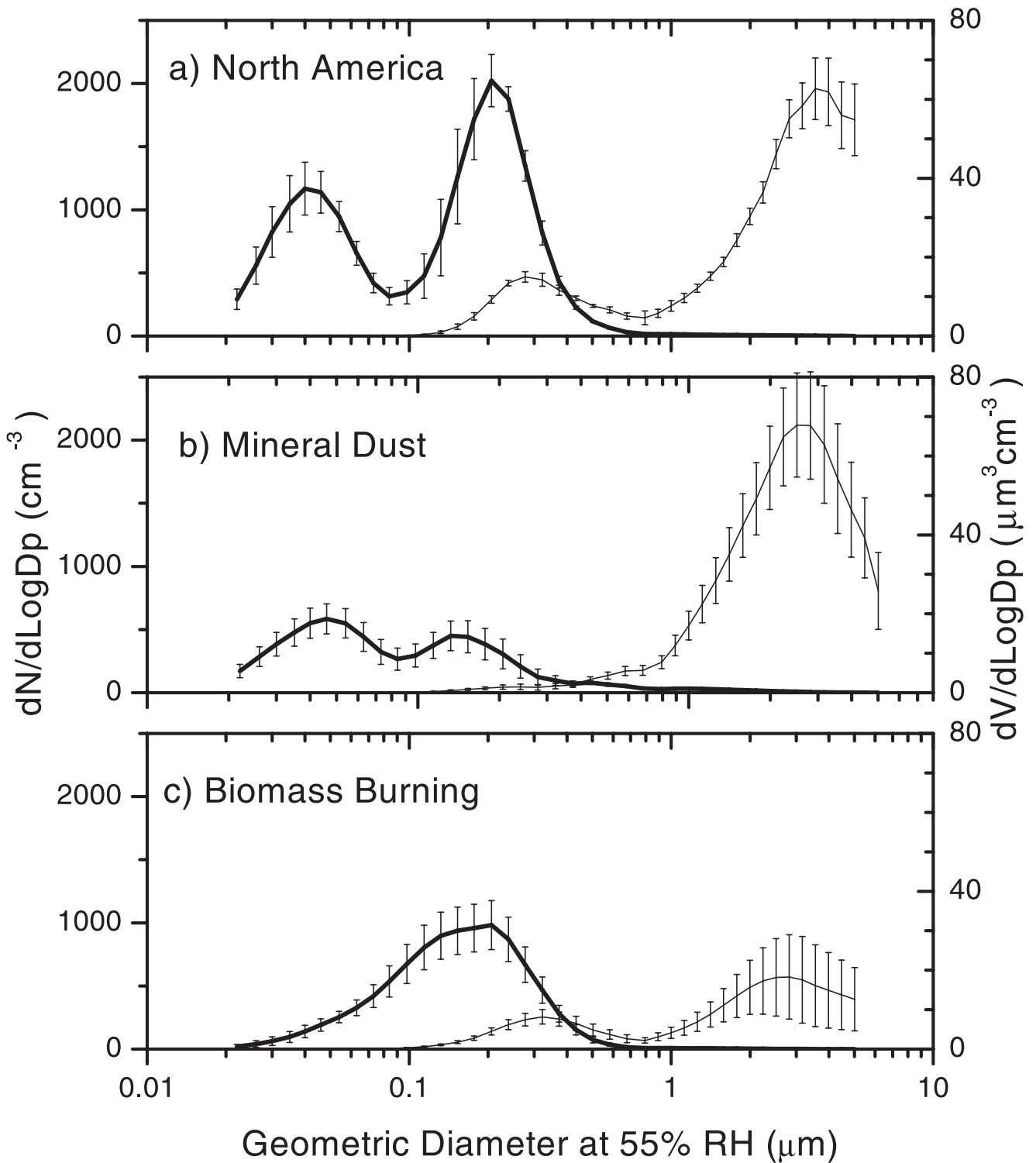


Figure 5. Number (heavy line) and volume (light line) distributions at 55% RH for 3 Atlantic Ocean marine air mass source regions during Aerosols99. The vertical bars represent one standard deviation in the mean number or volume in that bin size over the averaging period (N. Hemisphere marine Tropical — 77 hr; S. Hemisphere marine Tropical — 87 hr; African S. Hemisphere marine extra-tropical — 43 hr).

orological transport, and the length of time the aerosols spent over the ocean. The highest aerosol number concentrations were found in the Mediterranean (≈ 5300 particles cm^{-3}) and Iberian Coastal (≈ 4200 particles cm^{-3}) air masses (Figures 8a, 8c; Table 1) which had one dominant

mode in the Aitken mode size range. These aerosols were sampled within one day along their trajectory from the coast and were likely produced from local point sources along the coast [Verner *et al.*, 2000]. On this timescale (≈ 0.5 –1 day) nucleation mode particles from the continent are depleted

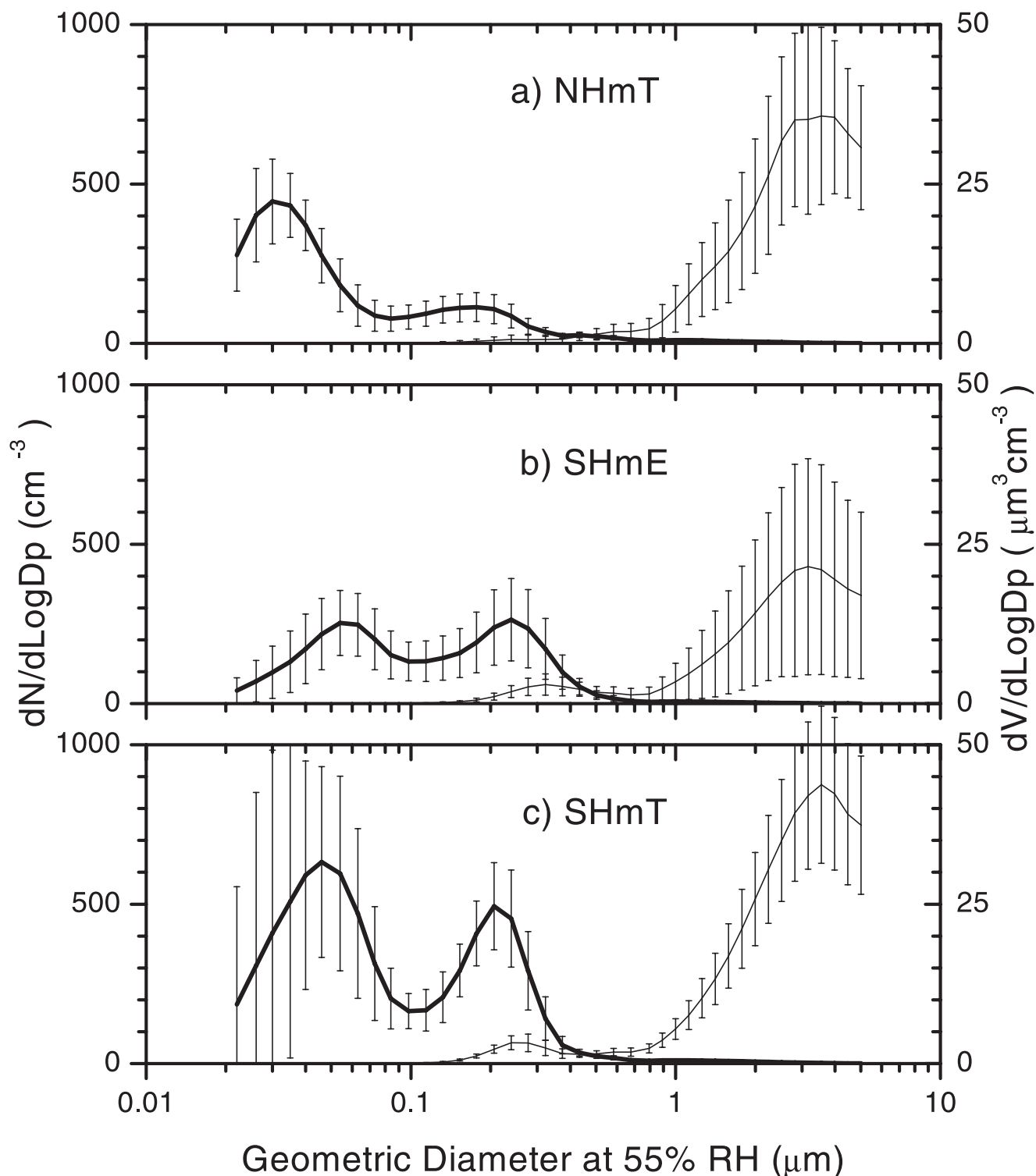


Figure 6. Number (heavy line) and volume (light line) distributions at 55% RH for 3 continental air mass source regions during Aerosols99. The vertical bars represent one standard deviation in the mean number or volume in that bin size over the averaging period (North America — 6 hr; African Mineral Dust — 48 hr; African Biomass Burning — 34 hr). Note the change in scale from other graphs for the volume distribution.

due to coagulation with larger particles [Hoppel *et al.*, 1990; Raes *et al.*, 2000] although SO_2 concentrations remain relatively high (e.g., 610 ± 410 ppt and 840 ± 760 ppt, in the Mediterranean and Iberian Coastal air masses respec-

tively [Bates *et al.*, 2000]). As these modified continental air masses continue to advect over the ocean entrainment of cleaner FT air dilutes the high concentrations of Aitken mode aerosol while conversion of dissolved SO_2 to sulfate

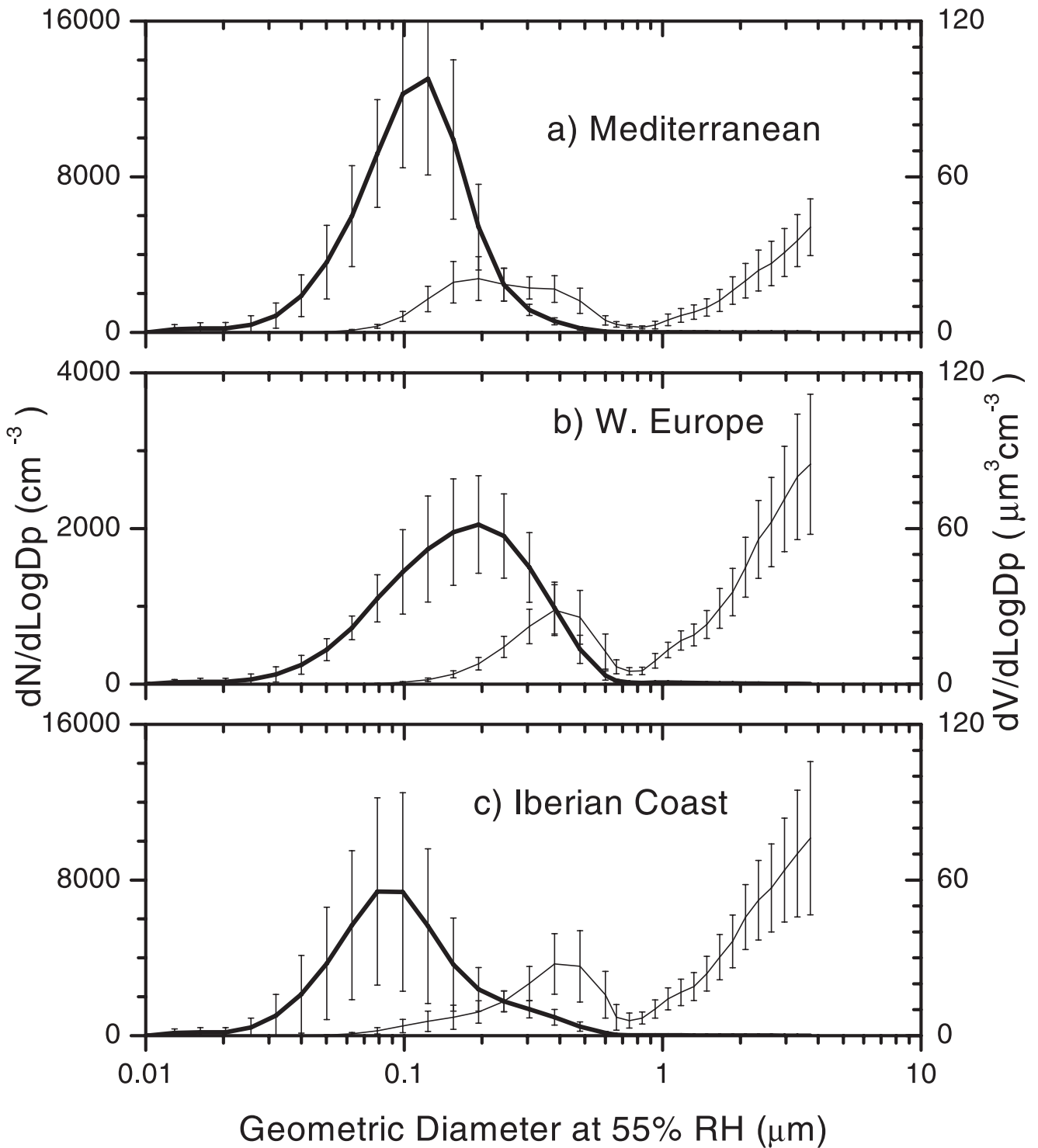


Figure 7. Number (heavy line) and volume (light line) distributions at 55% RH for 5 marine air mass source regions during ACE-1 and ACE-2. The vertical bars represent one standard deviation in the mean number or volume in that bin size over the averaging period (ACE-2 Atlantic Ocean N. Hemisphere marine Tropical — 75 hr; ACE-1 Pacific Ocean N. Hemisphere marine Tropical — 45 hr; ACE-1 Pacific Ocean S. Hemisphere marine Equatorial — 47 hr; ACE-1 Pacific Ocean S. Hemisphere marine Tropical — 65 hr; ACE-1 Southern Ocean S. Hemisphere marine extra-tropical — 475 hr). Note the change in scale for the ACE-2 number size distribution.

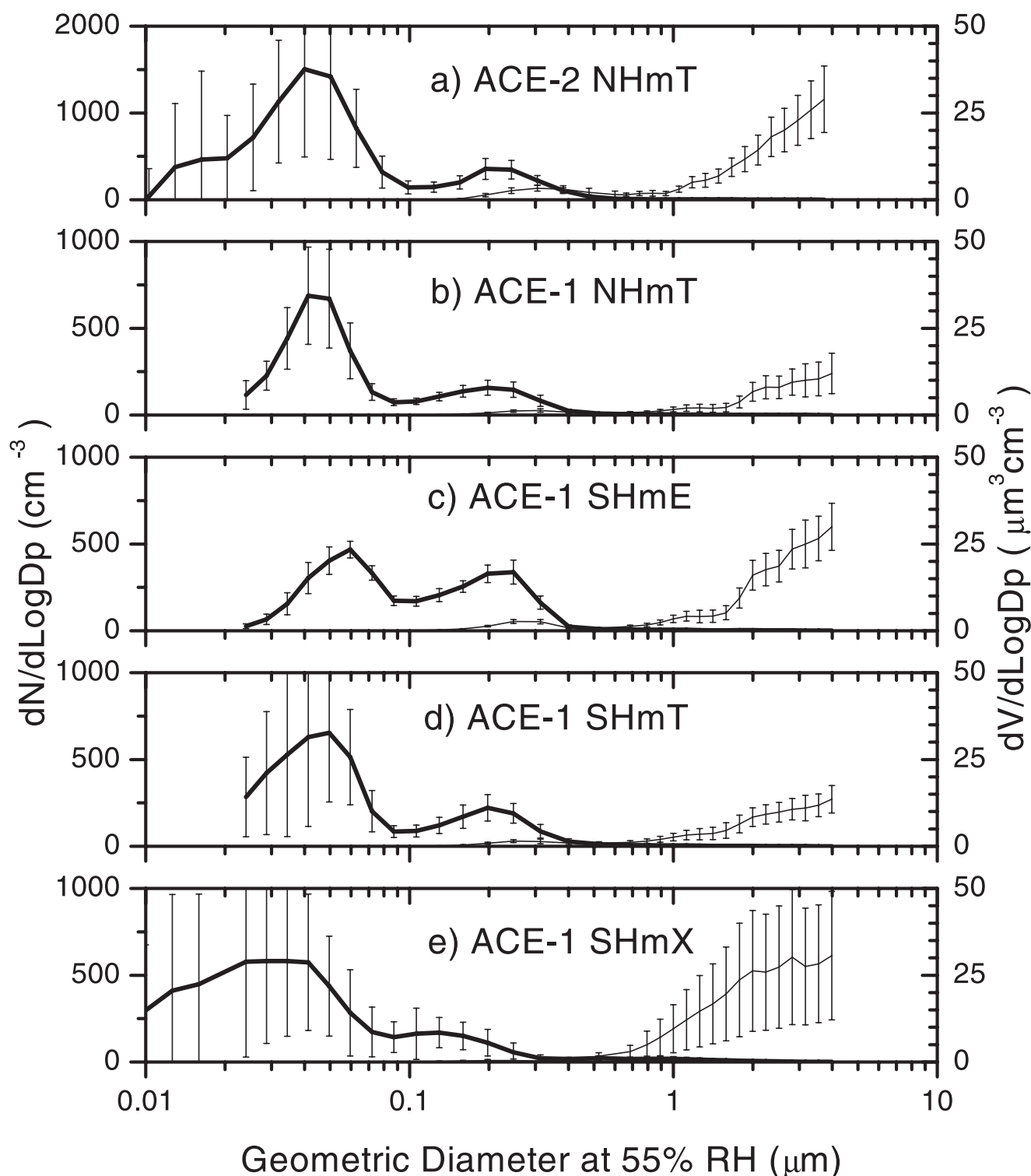


Figure 8. Number (heavy line) and volume (light line) distributions at 55% RH for 3 Atlantic Ocean continental air mass source regions during ACE-2. The vertical bars represent one standard deviation in the mean number or volume in that bin size over the averaging period (Iberian Coast — 114 hr; W. Europe — 41 hr; Mediterranean — 23 hr).

within cloud droplets depletes the remaining gaseous SO_2 and adds mass to the accumulation mode [Fitzgerald *et al.*, 1998; Osborne *et al.*, 2000]. The Western European air mass sampled off the coast of Portugal during ACE-2 (Figure 8b), for example, had been over the ocean for ≈ 3

days. The SO_2 concentrations (<100 ppt [Bates *et al.*, 2000]) and aerosol total number concentrations (≈ 1400 particles cm^{-3} , Table 1) were much lower than in the Mediterranean and Iberian Coastal air masses although the accumulation mode volume was the same as the Iberian

Coastal air mass (Table 1). Calculated 6-day back trajectories arriving at the ship's position above the MBL were from the mid Atlantic Ocean presumably providing cleaner FT air to dilute the continental MBL aerosol number concentration. Satellite imagery shows broken clouds along the 3-day MBL back trajectory. Although the 3-day transit over the partly cloud-covered ocean likely included some cloud processing (i.e., cloud activation, in-cloud chemical reactions and re-evaporation [Hoppel *et al.*, 1986; Raes *et al.*, 2000]), no clear minimum between the Aitken and accumulation modes developed on this timescale.

[30] In contrast, cloud processing was clearly evident in the North American air mass sampled during Aerosols99 (Figure 6a). This air mass had been over the ocean for ≈ 5 days. Based on the high number concentration in the accumulation mode ($520 \text{ particles cm}^{-3}$) compared with the adjacent NHmT air mass ($65 \text{ particles cm}^{-3}$), the North American air mass still retained a significant continental aerosol volume (Figure 6a) despite the 5 day transit and cloud processing.

[31] The aerosol number size distributions in the Atlantic (Figure 6b) and Indian (Figure 3b) Ocean air masses containing mineral dust were very similar. Both had relatively small diameter Aitken ($\approx 0.048 \mu\text{m}$) and accumulation ($\approx 0.14 \mu\text{m}$) modes however the Indian Ocean total number was significantly higher (1100 cm^{-3} versus 370 cm^{-3}). Although both air masses contained a significant submicron crustal component ($\approx 28\%$ in the Indian Ocean and $\approx 35\%$ in the Atlantic [Quinn *et al.*, 2001, 2002]), the air mass from Arabia also contained a large organic carbon component ($\approx 20\%$ [Quinn *et al.*, 2002]) from fossil fuel combustion (S. A. Guazzotti *et al.*, Characterization of pollution outflow from India and Arabia: Biomass burning and fossil fuel combustion, submitted to *Journal of Geophysical Research*, 2001). In both cases the back trajectories indicate a 2–3 day transit in the MBL from the coast to the ship with patchy cumulus clouds in the Atlantic and clear skies in the Indian Oceans. The small diameter accumulation modes suggest little aerosol growth during this period. Over the Atlantic, the calculated 6-day back trajectories arriving at the ship's position above the MBL were from the mid Atlantic Ocean. This could have been the source of the small-diameter Aitken mode with enhanced vertical mixing in the patchy cumulus clouds. The source of the small-diameter Aitken mode particles in the Arabian air mass is less clear. Possible sources include coagulation of nucleation mode particles from fossil fuel combustion or FT aerosol from the strongly subsiding back trajectories over the Arabian Peninsula.

[32] The biomass burning air mass sampled over the Atlantic during Aerosols99 was unusual in that it was transported out over the ocean in the FT and mixed down to the MBL in the ITCZ [Bates *et al.*, 2001]. There was no clear separation between the Aitken and accumulation modes (Figure 6c) suggesting minimal cloud processing. The modal diameters ($\approx 0.090 \mu\text{m}$ and $0.190 \mu\text{m}$) however are consistent with an approximate two day transport over the ocean and dilution by cleaner marine air, in this case from the MBL.

4. Conclusions

[33] The aerosol number and volume size distributions measured during four field campaigns in the Pacific, Atlan-

tic, and Indian Oceans reflected the source regions, meteorological transport, and the length of time the aerosols spent over the ocean. Although the measurements were not conducted in a Lagrangian framework, the regional aerosol characteristics, combined with calculated air mass back trajectories, provide information on the dominant processes and timescales that shape the aerosol size distributions over the ocean. In marine air masses (>6 days over the ocean) the ratio of the Aitken mode number to the accumulation mode number generally decreased from the high latitudes to the subtropics to the equator reflecting increasing aerosol residence time in the MBL (from approximately one day to 10 days). The aerosol volume was always dominated by the coarse mode seasalt.

[34] Modified continental aerosols measured near the aerosol source regions (<1 day from the coast) off the coast of Europe (Figures 8a, 8c) had one dominant mode in the number distribution in the Aitken mode size range. Continental aerosols sampled after a 2–3 days transit from the coasts of Europe (Figure 8b), Africa (Figure 6c), and India (Figure 3a) were more broadly distributed, encompassing the Aitken and accumulation mode size ranges. Dilution by entrainment from the FT combined with coagulation and condensation most likely decreased the aerosol number while increasing aerosol diameter. The air masses containing mineral dust in the Atlantic (Figure 6b) and Indian Oceans (Figure 3b) still had small diameter Aitken and accumulation modes after a 2–3 day transit over the ocean. We speculate that the FT provided the Aitken mode through entrainment and that low concentrations of gases and soluble aerosol limited growth by coagulation and condensation.

[35] Continental aerosols sampled after a 5–6 day transit over the ocean were further modified depending upon the extent of cloud cover. In regions with extensive cloud processing, the continental aerosol distribution evolved into a marine-like distribution, although still with higher number and volume concentrations (Figure 6a) than “background” marine conditions ($200\text{--}300 \text{ particles cm}^{-3}$ in the subtropical and equatorial regions). In regions without or with minimal cloud processing of the continental aerosol, there was no clear distinction between the Aitken and accumulation modes (Figures 3d, 3e). On times scales of 6 days, the Aitken mode decreased through coagulation as the overall aerosol increased in diameter.

[36] Although continental aerosols over the ocean have a major impact on the aerosol number concentration, the aerosol volume is still generally dominated by coarse mode sea salt (e.g., ACE-2 [Quinn *et al.*, 2000]). There are exceptions. In regions where mineral dust is transported over the ocean, the coarse mode mineral dust can significantly add to the coarse mode sea salt volume ($\approx 50\%$ in Aerosols99 [Bates *et al.*, 2001] and INDOEX [Quinn *et al.*, 2002]). In regions of low wind speeds (IndSub — $3.5 \pm 0.88 \text{ m/s}$, AS/CI — $4.7 \pm 2.2 \text{ m/s}$, BoB — $2.3 \pm 0.79 \text{ m/s}$) and high modified continental aerosol concentrations the accumulation mode (primarily ammonium sulfate [Quinn *et al.*, 2002]) can dominate the volume distribution (Figures 3a, 3e).

[37] Intercalibrated data sets, with well-characterized inlets and measurement humidities, are essential for refining GCMs and satellite retrieval algorithms. The aerosol num-

ber and volume distributions reported here add to the growing database of MBL aerosol measurements [Heintzenberg *et al.*, 2000]. However, it is clear from these data that regional aerosol properties are highly dependent upon the local meteorology and related air mass back trajectories, especially in areas influenced by continental aerosols. In high latitudes marine aerosol distributions also vary seasonally [Ayers and Gras, 1991] due to oceanic emissions of dimethylsulfide. Gridded MBL aerosol data sets thus must take into account regional and seasonal meteorological patterns and biological processes to provide the aerosol parameters needed for comparison with GCMs and satellite retrieval algorithms.

[38] **Acknowledgments.** We thank the officers and crew of NOAA R/V *Ronald H. Brown* for their cooperation and support. We also thank James Johnson, Stephan Leinert, Andreas Nowak, and Alfred Wiedensohler for their assistance with the data. This research was funded by the Aerosol Project of the NOAA Climate and Global Change Program, the NOAA Office of Oceanic and Atmospheric Research, and the NASA Global Aerosol Climatology Project. This is NOAA/PMEL contribution 2352 and JISAO contribution 843.

References

- Ayers, G. P., and J. L. Gras, Seasonal relationship between cloud condensation nuclei and aerosol methanesulfonate in marine air, *Nature*, 353, 834–835, 1991.
- Bates, T. S., B. J. Huebert, J. L. Gras, F. B. Griffiths, and P. A. Durkee, International Global Atmospheric Chemistry (IGAC) Project's First Aerosol Characterization Experiment (ACE 1): Overview, *J. Geophys. Res.*, 103, 16,297–16,318, 1998a.
- Bates, T. S., V. N. Kapustin, P. K. Quinn, D. S. Covert, D. J. Coffman, C. Mari, P. A. Durkee, W. DeBruyn, and E. Saltzman, Processes controlling the distribution of aerosol particles in the lower marine boundary layer during the First Aerosol Characterization Experiment (ACE 1), *J. Geophys. Res.*, 103, 16,369–16,383, 1998b.
- Bates, T. S., P. K. Quinn, D. S. Covert, D. J. Coffman, J. E. Johnson, and A. Wiedensohler, Aerosol physical properties and processes in the lower marine boundary layer: A comparison of shipboard sub-micron data from ACE 1 and ACE 2, *Tellus*, 52, 258–272, 2000.
- Bates, T. S., P. K. Quinn, D. J. Coffman, J. E. Johnson, T. L. Miller, D. S. Covert, A. Wiedensohler, S. Leinert, A. Nowak, and C. Neusüß, Regional physical and chemical properties of the marine boundary layer aerosol across the Atlantic during Aerosols99: An overview, *J. Geophys. Res.*, 106, 20,767–20,782, 2001.
- Berg, O. H., E. Swietlicki, and R. Krejci, Hygroscopic growth of aerosol particles in the marine boundary layer over the Pacific and Southern Oceans during the First Aerosol Characterization Experiment (ACE 1), *J. Geophys. Res.*, 103, 16,535–16,546, 1998.
- Clarke, A. D., S. Howell, P. K. Quinn, T. S. Bates, J. A. Ogren, E. Andrews, A. Jefferson, and A. Massling, INDOEX aerosol: A comparison and summary of chemical, microphysical and optical properties observed from land, ship, and aircraft, *J. Geophys. Res.*, 107, 10.1029/2001JD000572, in press, 2002.
- Covert, D. S., V. N. Kapustin, T. S. Bates, and P. K. Quinn, Physical properties of marine boundary layer aerosol particles of the mid-Pacific in relation to sources and meteorological transport, *J. Geophys. Res.*, 101, 6919–6930, 1996.
- Covert, D. S., A. Wiedensohler, and L. M. Russell, Particle charging and transmission efficiencies of aerosol charge neutralizers, *Aerosol Sci. Technol.*, 27, 208–214, 1997.
- Draxler, R. R., Hybrid Single-Particle Lagrangian Integrated Trajectories (HY-SPLIT): Version 3.0. User's Guide and Model Description, *Tech. Rep. ERL ARL-195*, Natl. Oceanic and Atmos. Admin., Silver Spring, Md., 1992.
- Fitzgerald, J. W., J. J. Marti, W. A. Hoppel, G. M. Frick, and F. Gelbard, A one-dimensional sectional model to simulate multicomponent aerosol dynamics in the marine boundary layer, 2, Model application, *J. Geophys. Res.*, 103, 16,103–16,117, 1998.
- Hainsworth, A. H. W., A. L. Dick, and J. L. Gras, Climatic context of the First Aerosol Characterization Experiment (ACE 1): A meteorological and chemical overview, *J. Geophys. Res.*, 103, 16,319–16,340, 1998.
- Heintzenberg, J., D. C. Covert, and R. Van Dingenen, Size distribution and chemical composition of marine aerosols: a compilation and review, *Tellus, Ser. B*, 52, 1104–1122, 2000.
- Hoppel, W. A., J. W. Fitzgerald, G. M. Frick, R. E. Larson, and E. J. Mack, Aerosol size distributions and optical properties found in the marine boundary layer over the Atlantic Ocean, *J. Geophys. Res.*, 95, 3659–3686, 1990.
- Hoppel, W. A., G. M. Frick, and R. E. Larson, Effect of nonprecipitating clouds on the aerosol size distribution in the marine boundary layer, *Geophys. Res. Lett.*, 13, 125–128, 1986.
- King, M. D., Y. J. Kaufman, D. Tanre, and T. Nakajima, Remote sensing of tropospheric aerosols from space: past, present, and future, *Bull. Am. Meteorol. Soc.*, 80, 2229–2259, 1999.
- Livingston, J. M., et al., Shipboard sunphotometer measurements of aerosol optical depth spectra and columnar water vapor during ACE-2 and comparison with selected land, ship, aircraft, and satellite measurements, *Tellus*, 52, 593–618, 2000.
- Osborne, S. R., et al., Evolution of the aerosol, cloud and boundary layer dynamic and thermodynamic characteristics during the second Lagrangian experiment of ACE-2, *Tellus*, 52, 375–400, 2000.
- Quinn, P. K., T. S. Bates, D. J. Coffman, T. L. Miller, J. E. Johnson, D. S. Covert, J. P. Putaud, C. Neususs, and T. Novakov, A comparison of aerosol chemical and optical properties from the First and Second Aerosol Characterization Experiments, *Tellus*, 52, 238–257, 2000.
- Quinn, P. K., D. J. Coffman, V. N. Kapustin, T. S. Bates, and D. S. Covert, Aerosol optical properties in the marine boundary layer during ACE 1 and the underlying chemical and physical aerosol properties, *J. Geophys. Res.*, 103, 16,547–16,563, 1998.
- Quinn, P. K., D. J. Coffman, T. S. Bates, T. L. Miller, J. E. Johnson, K. Voss, E. J. Welton, and C. Neusüß, Dominant aerosol chemical components and their contribution to extinction during the Aerosols99 cruise across the Atlantic, *J. Geophys. Res.*, 106, 20,783–20,809, 2001.
- Quinn, P. K., D. J. Coffman, T. S. Bates, T. L. Miller, J. E. Johnson, E. J. Welton, C. Neusüss, M. Miller, and P. J. Sheridan, Aerosol optical properties during INDOEX 1999: Means, variability, and controlling factors, *J. Geophys. Res.*, 107, 10.1029/2000JD000037, in press, 2002.
- Raes, R., R. Van Dingenen, E. Vignati, J. Wilson, J. P. Putaud, J. H. Seinfeld, and P. Adams, Formation and cycling of aerosols in the global troposphere, *Atmos. Environ.*, 34, 4215–4240, 2000.
- Ramanathan, V., et al., Indian Ocean Experiment: An integrated analysis of the climate forcing and effects of the great Indo-Asian haze, *J. Geophys. Res.*, 106, 28,371–28,398, 2001.
- Stratman, F., and A. Wiedensohler, A new data inversion algorithm for DMPS measurements, *J. Aerosol Sci.*, 27, 339–340, 1997.
- Swietlicki, E., et al., Hygroscopic properties of aerosol particles in the north-eastern Atlantic during ACE-2, *Tellus, Ser. B*, 52, 201–227, 2000.
- Verner, G., F. Raes, D. Vogelezang, and D. Johnson, The 2nd Aerosol Characterization Experiment (ACE-2): Meteorological and chemical context, *Tellus, Ser. B*, 52, 126–140, 2000.
- Weber, R. J., P. H. McMurry, L. Mauldin, D. J. Tanner, F. L. Eisele, F. J. Brechtel, S. M. Kreidenweis, G. L. Kok, R. D. Schillawski, and D. Baumgardner, A study of new particle formation and growth involving biogenic trace gas species measured during ACE-1, *J. Geophys. Res.*, 104, 21,673–21,684, 1999.
- Wiedensohler, A., et al., Intercomparison study of the size-dependent counting efficiency of 26 condensation particle counters, *Aerosol Sci. Technol.*, 27, 224–254, 1997.
- Winklmayr, W., G. P. Reischl, A. O. Lindner, and A. Berner, A new electromobility spectrometer for the measurement of aerosol size distributions in the size range from 1 to 1000 nm, *J. Aerosol Sci.*, 22, 289–296, 1991.

T. S. Bates, D. J. Coffman, and P. K. Quinn, NOAA/Pacific Marine Environmental Laboratory (PMEL), 7600 Sand Point Way NE, Seattle, WA 98115, USA. (bates@pmel.noaa.gov)

D. S. Covert, The Joint Institute for the Study of the Atmosphere and Ocean (JISAO), University of Washington, Seattle, WA, USA.